

DISCOVERY OF A DETACHED, ECLIPSING 40 MIN PERIOD DOUBLE WHITE DWARF BINARY AND A FRIEND: IMPLICATIONS FOR HE+CO WHITE DWARF MERGERS *

WARREN R. BROWN,¹ MUKREMIN KILIC,² ALEKZANDER KOSAKOWSKI,² AND A. GIANNINAS²

¹*Smithsonian Astrophysical Observatory, 60 Garden St, Cambridge, MA 02138 USA*

²*Homer L. Dodge Department of Physics and Astronomy, University of Oklahoma, 440 W. Brooks St., Norman, OK, 73019 USA*

(Accepted August 16, 2017)

ABSTRACT

We report the discovery of two detached double white dwarf (WD) binaries, SDSS J082239.546+304857.19 and SDSS J104336.275+055149.90, with orbital periods of 40 and 46 min, respectively. The 40 min system is eclipsing; it is composed of a $0.30 M_{\odot}$ and a $0.52 M_{\odot}$ WD. The 46 min system is a likely *LISA* verification binary. The short 20 ± 2 Myr and ~ 34 Myr gravitational wave merger times of the two binaries imply that many more such systems have formed and merged over the age of the Milky Way. We update the estimated Milky Way He+CO WD binary merger rate and affirm our previously published result: He+CO WD binaries merge at a rate at least 40 times greater than the formation rate of stable mass-transfer AM CVn binaries, and so the majority must have unstable mass-transfer. The implication is that spin-orbit coupling in He+CO WD mergers is weak, or perhaps nova-like outbursts drive He+CO WDs into merger as proposed by Shen.

Keywords: binaries: close — Galaxy: stellar content — white dwarfs

wbrown@cfa.harvard.edu, kilic@ou.edu, alexg@nhn.ou.edu

* Based on observations obtained at the MMT Observatory, a joint facility of the Smithsonian Institution and the University of Arizona, and on observations obtained with the Apache Point Observatory 3.5-meter telescope, which is owned and operated by the Astrophysical Research Consortium.

1. INTRODUCTION

There are about 100 double degenerate white dwarf (WDs) binaries known with orbital periods less than about 1 d (e.g. Saffer et al. 1988; Bragaglia et al. 1990; Marsh et al. 1995; Moran et al. 1997; Maxted et al. 2000; Morales-Rueda et al. 2005; Nelemans et al. 2005; Vennes et al. 2011; Brown et al. 2016a; Rebassa-Mansergas et al. 2017; Breedt et al. 2017; Kilic et al. 2017). Short-period WD binaries with periods less than 1 h have gravitational wave merger times less than about 100 Myr, and thus are interesting gravitational wave sources at mHz frequencies (Nelemans 2009; Marsh 2011; Nissanke et al. 2012). The 765 sec orbital period binary J0651 (Brown et al. 2011), for example, should be detected by the proposed *LISA* gravitational wave detector shortly after it is turned on (Korol et al. 2017). Short-period WD binaries are also interesting because they must either evolve into stable AM CVn systems, explode as supernovae, or merge into single massive WDs, R CrB stars, and related objects (e.g. Webbink 1984; Iben 1990). None of these transformations have been observed directly, but we can compare WD merger rates with different formation rates to constrain their outcome.

Here, we report the discovery of two detached, double WD binaries, SDSS J082239.546+304857.19 and SDSS J104336.275+055149.90, with orbital periods of 40 and 46 min, respectively. We will henceforth refer to these objects as J0822 and J1043. J0822 and J1043 are the 5th- and 6th-shortest period WD binaries discovered by our Extremely Low Mass (ELM) Survey, a targeted spectroscopic survey for extremely low mass $\approx 0.2 M_{\odot}$ He-core WDs (Brown et al. 2016a, and references therein). Thus we refer to degenerate $\approx 0.2 M_{\odot}$ objects as ELM WDs. Practically all ELM WDs are observed in compact binaries, with typical $M_2 = 0.76 \pm 0.25 M_{\odot}$ WD companions and median $P = 5.5$ h periods (Brown et al. 2016a). J0822 and J1043 bring our ELM Survey sample to 82 binaries, more than half of which have merger times less than a Hubble time.

Eclipses provide accurate constraints on the physical parameters of binaries. J0822 is the seventh eclipsing double WD binary known after NLTT 11748 (Steinfadt et al. 2010), CSS 41177 (Drake et al. 2010; Parsons et al. 2011), GALEX J1717 (Vennes et al. 2011), SDSS J0651 (Brown et al. 2011), SDSS J0751 (Kilic et al. 2014b), and SDSS J1152 (Hallakoun et al. 2016). J0822 has a total mass of $0.82 M_{\odot}$, a mass ratio of about 1:2, and will merge in 20 Myr.

The existence of double WD binaries with ~ 10 Myr merger times implies that many more such systems have

formed and evolved over the age of the Milky Way. Conversely, longer period systems remain binaries for the age of the Milky Way and must accumulate in observed samples. An obvious question is what merging ELM WD binaries like J0822 and J1043 become.

Previously, we used the magnitude-limited ELM Survey to estimate the local space density of ELM WD binaries and then calculate their merger rate by 1) inverting the distribution of merger times and 2) by forward-modeling different trial distributions to match the observations. The major source of uncertainty comes from the small number statistics of rapidly merging binaries. The gravitational wave merger timescale depends most strongly on orbital period (Kraft et al. 1962), so the shortest-period binaries dominate the merger rate estimate. Given that J0822 and J1043 increase the sample of $P < 1$ h ELM WD binaries by 40%, we revisit the merger rate estimate in light of the new discoveries.

We begin by presenting our spectroscopic and photometric observations of J0822 and J1043. We fit stellar atmosphere models to the spectra, orbital parameters to the radial velocities, and light curve parameters to the photometry. The Galactic kinematics of the binaries suggest that J0822 is a halo object while J1043 is a thin disk object. We discuss the mass and mass ratio of J0822 in the context of other eclipsing double WD binaries, and close with an update on the merger rate of He+CO WD binaries in the Milky Way.

2. DATA

2.1. Target Selection

The ELM Survey is a spectroscopic survey of low mass WD candidates selected on the basis of broadband color (Brown et al. 2012). We have also targeted some objects on the basis of stellar atmosphere fits to pre-existing Sloan Digital Sky (SDSS) spectra (Kilic et al. 2010, 2011a, 2014a). J0822 is an example of an object identified from its SDSS spectrum. In 2016 February we obtained a pair of spectra to validate its nature and test for radial velocity variability. We followed-up J0822 with time-series spectroscopy in 2016 October and 2017 March to determine its orbit.

We targeted J1043 as part of the main ELM Survey (Brown et al. 2012). A single spectrum obtained in 2014 April identified J1043 as a likely low mass WD; a pair of spectra obtained in 2016 February revealed J1043 is velocity variable. We re-observed J1043 with time-series spectroscopy in 2016 December and 2017 March. The year-long observing time baseline for both objects provide strong orbital period constraints using radial velocity alone.

2.2. Spectroscopy

We obtain spectra in the same way as described in previous ELM Survey papers. In brief, we use the 6.5m MMT telescope Blue Channel spectrograph with the 832 l mm^{-1} grating in 2nd order, providing us with 1 \AA spectral resolution over $3600 < \lambda < 4500 \text{ \AA}$. We pair all spectra with comparison lamp exposures for accurate wavelength calibration. We measure radial velocities with the cross-correlation package RVSAO (Kurtz & Mink 1998). We adjust exposure times to observing conditions, and obtain median 35 km s^{-1} errors for J0822 using exposure times between 12 and 22 min. J1043 is a brighter target, and we obtain median 20 km s^{-1} radial velocity errors using exposure times between 6.5 and 9 min. We became concerned about the length of our exposure times after we discovered the velocities were phasing at $\approx 45 \text{ min}$ periods.

To properly sample the phase curves and validate the short orbital periods, we obtained 1.5 h worth of back-to-back spectra for both objects at 2 \AA resolution (with the MMT Blue Channel spectrograph 800 l mm^{-1} grating in 1st order) using half the normal exposure times. The radial velocity uncertainties are worse with this setup, however the time series confirm the $\approx 45 \text{ min}$ periods.

In total, we obtained 20 spectra of J0822 and 31 spectra of J1043. We provide the radial velocities in a Data behind the Figure table accessible in the on-line journal. Both objects are observed to be single-lined spectroscopic binaries, as seen in Figure 1.

2.3. High-Speed Photometry

We obtained time-series photometry for J0822 and J1043 using the Apache Point Observatory 3.5m telescope with the Agile frame-transfer camera (Mukadam et al. 2011) and the BG40 filter on the night of UT 2 March 2017. We use exposure times of 30 s for J0822 and 15 s for J1043, and obtain total integrations of 68 min and 60 min, respectively. There is a 5.6 min gap in the J0822 data due to an instrument problem.

We use standard IRAF¹ routines to perform aperture photometry. We correct for transparency variations using two relatively bright comparison stars in the field of view of each WD. After detecting eclipses in J0822, we attempted additional follow-up on three different nights. All follow-up attempts were unfortunately lost to weather.

¹ IRAF is distributed by the National Optical Astronomy Observatories, which are operated by the Association of Universities for Research in Astronomy, Inc., under cooperative agreement with the National Science Foundation.

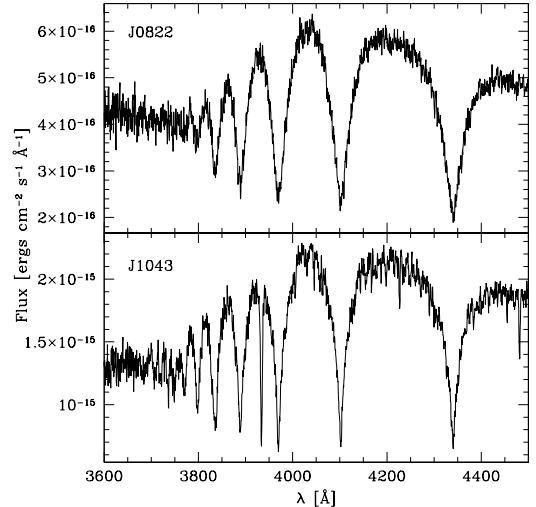


Figure 1. Summed rest-frame spectra of J0822 (top panel) and J1043 (bottom panel).

3. ANALYSIS AND RESULTS

3.1. Stellar Atmosphere Fits

We perform stellar atmosphere fits in the same way as described in previous ELM Survey papers. In brief, we fit the summed, rest-frame spectra to a grid of pure hydrogen atmosphere models that span $4,000 \text{ K} < T_{\text{eff}} < 35,000 \text{ K}$ and $4.5 < \log g < 9.5$ (Gianninas et al. 2011, 2014, 2015) and that include the Stark broadening profiles from Tremblay & Bergeron (2009). J1043 has a temperature and gravity that require three-dimensional stellar atmosphere model corrections, which reduce the 1D parameters by 230 K and 0.23 dex (Tremblay et al. 2015). We present the corrected parameters in Table 1.

J1043 is also a DAZ WD that exhibits strong Ca II $\lambda 3933$ and Mg II $\lambda 4481$ absorption lines (Figure 1). The Ca II and Mg II lines show the same radial velocity variability as measured from the Balmer lines, and so must come from the WD. We and others regularly see Ca II in other $\log g \sim 6$ ELM WD spectra (Brown et al. 2013; Kaplan et al. 2013). We mask the region around Ca II when doing the Balmer line fits.

3.2. White Dwarf Parameters

We estimate WD mass and luminosity by matching the measured T_{eff} and $\log g$ to the ELM WD evolutionary tracks of Istrate et al. (2016). The tracks account for the effects of element diffusion and rotation mixing, beginning at the moment the progenitor detaches from the mass-transfer phase. Progenitor metallicity can have a significant impact on the hydrogen envelope mass, the number of thermonuclear shell flashes, and the resulting cooling time of the tracks (Althaus et al. 2015). Thus we

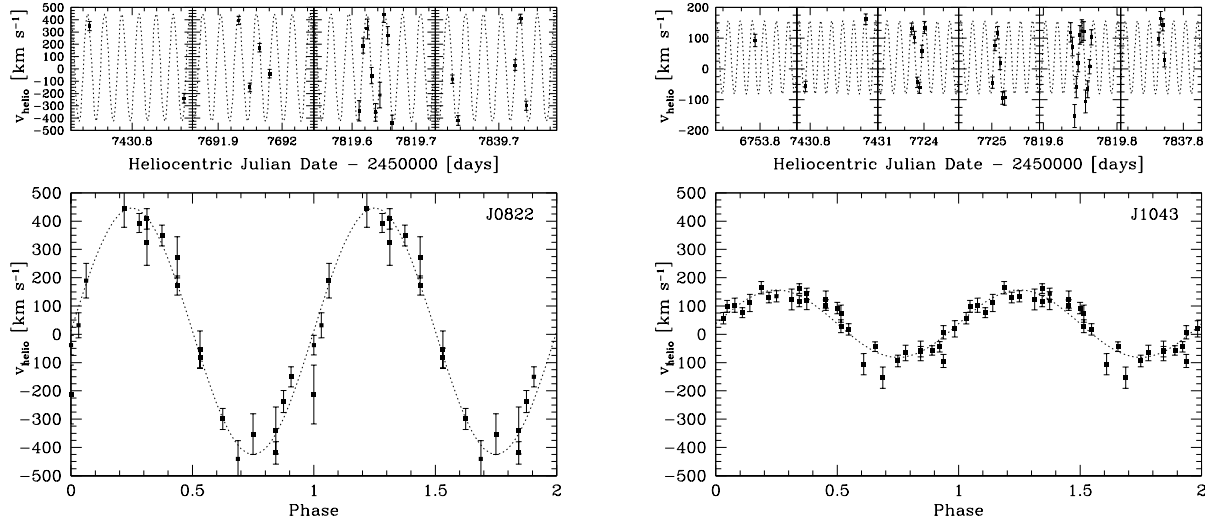


Figure 2. Radial velocity observations of J0822 and J1043. Nightly measurements are plotted in the small panels; measurements phased to the χ^2 minima at $P = 0.028126$ d and $P = 0.032618$ d, respectively, are plotted in the large panels. The radial velocities are available as the Data behind the Figure.

apply $Z = 0.02$ tracks to disk objects, and $Z = 0.001$ tracks to halo objects. As a cross-check, we compare with Althaus et al. (2013) solar metallicity tracks.

We interpolate the evolutionary tracks in the same way as described in previous ELM Survey papers. Our approach is to identify the two nearest tracks to an observed T_{eff} and $\log g$ value, and interpolate between the tracks on the basis of $\log g$. Loops due to shell flashes complicate the picture, and so we re-sample T_{eff} and $\log g$ with their errors to estimate the dispersion of the mass and luminosity estimates. The results are presented in Table 1.

J0822 has mass $M_1 = 0.304 \pm 0.014 M_{\odot}$ and absolute g -band magnitude $M_g = +9.96 \pm 0.09$ based on Istrate et al. (2016) $Z = 0.001$ tracks. With a de-reddened apparent magnitude $g_0 = 20.198 \pm 0.023$, J0822 is 1.11 kpc distant and likely a halo object (see below).

J1043, on the other hand, has $M_1 = 0.183 \pm 0.010 M_{\odot}$ and $M_g = +10.23 \pm 0.11$ mag based on Istrate et al. (2016) $Z = 0.02$ tracks. With a de-reddened apparent magnitude $g_0 = 19.054 \pm 0.017$, J1043 is 0.58 kpc distant and likely a disk object (see below). Mass and luminosity estimates from Althaus et al. (2013) tracks agree to within $1\text{-}\sigma$ for both objects, thus the mass and luminosity estimates appear robust to the choice of evolutionary tracks.

Interestingly, the evolutionary tracks predict that J1043 has undergone multiple thermonuclear shell flashes, while J0822 has not. Istrate et al. (2016) argue that rotational mixing can keep metals visible at the surface of a WD for longer-than-expected periods

of time after shell flashes. This prediction is consistent with the strong metal lines present in J1043 and absent in J0822.

3.3. Disk / Halo Kinematics

We use kinematics to determine whether the objects belong to the disk or halo. The gravitational redshift corrections for J0822 and J1043 are 7.9 ± 0.3 and 3.3 ± 0.2 km s $^{-1}$, respectively. The objects have comparable systemic radial velocities, $\gamma_{\text{J0822}} = 10.2 \pm 23.0$ km s $^{-1}$ and $\gamma_{\text{J1043}} = 31.7 \pm 4.6$ km s $^{-1}$, but different proper motions.

We obtain proper motions from the HSOY catalog (Altmann et al. 2017), a new proper motion catalog that uses *Gaia* Data Release 1 positions for its final epoch. While J0822 is not detected in all epochs, its proper motion $\mu_{\text{J0822}} = 29.7 \pm 7.9$ mas yr $^{-1}$ is formally significant. J1043 is detected in all epochs and has a smaller proper motion, $\mu_{\text{J1043}} = 8.5 \pm 3.6$ mas yr $^{-1}$.

We calculate velocities in the Galactic rest frame assuming a circular velocity of 235 km s $^{-1}$ and the Local Standard of Rest motion of Schönrich et al. (2010). We use Chiba & Beers (2000) velocity ellipsoid values to put the motions in context. J0822’s space motion, $(U, V, W) = (8 \pm 25, -141 \pm 31, -29 \pm 28)$ km s $^{-1}$, falls outside the $2\text{-}\sigma$ velocity dispersion threshold of the thick disk, but lies well within the $1\text{-}\sigma$ velocity dispersion threshold of the halo. On this basis, we identify J0822 as a likely halo object. J1043’s space motion, $(U, V, W) = (-20 \pm 7, -6 \pm 7, 24 \pm 6)$ km s $^{-1}$, is con-

Table 1. System Parameters

Parameter	J0822	J1043
RA (J2000)	8:22:39.546	10:43:36.275
Dec (J2000)	+30:48:57.19	+5:51:49.90
T_{eff} (K)	13920 ± 255	9260 ± 140
$\log g$	7.14 ± 0.05	6.60 ± 0.06
M_1 (M_{\odot})	0.304 ± 0.014	0.183 ± 0.010
M_g (mag)	$+9.96 \pm 0.09$	$+10.23 \pm 0.11$
g_0 (mag)	20.198 ± 0.023	19.054 ± 0.017
d_{helio} (kpc)	1.11 ± 0.08	0.58 ± 0.05
P (d)	0.02797 ± 0.00016	0.03170 ± 0.00092
k (km s $^{-1}$)	415.7 ± 22.7	115.2 ± 6.8
γ (km s $^{-1}$)	10.2 ± 23.0	31.7 ± 4.6
M_2 (M_{\odot})	0.524 ± 0.050	> 0.07 (if 0.76 ± 0.25)
i (deg)	$88.1^{+1.4}_{-2.3}$	< 85.7 (then $12.6^{+2.9}_{-1.8}$)
a (R_{\odot})	0.364 ± 0.008	> 0.27 (and 0.41 ± 0.04)
τ_{merge} (Myr)	20 ± 2	< 240 (and 34^{+12}_{-7})
$\log h$	-22.36 ± 0.05	> -22.9 (and -21.7 ± 0.1)
R_1 (R_{\odot})	$0.022^{+0.015}_{-0.014}$...
R_2 (R_{\odot})	$0.0041^{+0.0082}_{-0.0037}$...
L_2/L_1	$0.00^{+0.04}_{-0}$...

sistent with the disk, and so we consider J1043 a likely disk object.

3.4. Binary Orbital Elements

We calculate orbital elements in a similar way as described in previous ELM Survey papers. In brief, we minimize χ^2 for a circular orbit following the code of [Kenyon & Garcia \(1986\)](#). To compare the model to the observations, we average the model over each exposure time as we search through period and phase. The time-baseline and phase coverage of the observations (Figure 2) yield a well-defined χ^2 minimum in both objects. We determine the best-fit parameters from the envelope of the χ^2 minima, which are symmetric but have sub-

structure due to our sampling. The orbital fits to J0822 and J1043 have reduced χ^2 of 1.06 and 1.17, respectively.

We estimate errors by re-sampling the velocities with their errors and re-fitting the orbital parameters 10,000 times. This Monte Carlo approach samples the χ^2 space in a self-consistent way. We report the median orbital parameters along with the averaged 15.9% and 84.1% percentiles of the distributions in Table 1. The systemic velocities are corrected for gravitational redshift.

Kepler's 3rd law, written as the binary mass function, relates orbital period P , semi-amplitude k , ELM WD mass M_1 , companion mass M_2 , and orbital inclination i as follows:

$$\frac{Pk^3}{2\pi G} = \frac{(M_2 \sin i)^3}{(M_1 + M_2)^2}. \quad (1)$$

We directly measure P and k . We derive M_1 from the observed T_{eff} and $\log g$. Given a constraint on i (i.e. from eclipses or another observational constraint), we can derive M_2 .

J0822 has $P = 40.28 \pm 0.23$ min and semi-amplitude $k = 415.7 \pm 22.7$ km s $^{-1}$. Assuming inclination $i = 88.1^{+1.4}_{-2.3}$ deg (see below), Kepler's 3rd Law tells us that J0822's unseen companion has mass $M_2 = 0.524 \pm 0.05$ M_{\odot} and orbital separation $a = 0.364 \pm 0.008$ R_{\odot} . J0822 is a double WD binary. The gravitational wave merger time of the binary is remarkably short, $\tau = 20 \pm 2$ Myr, however the gravitational wave strain is only $\log h = -22.36 \pm 0.05$ given the distance and masses involved. The eclipse light curve allows us to further characterize J0822 below.

J1043 has $P = 45.65 \pm 1.32$ min and $k = 115.2 \pm 6.8$ km s $^{-1}$. The larger period uncertainty reflects the broader envelope of its χ^2 minimum. In the absence of a constraint on inclination, Kepler's 3rd Law tells us that J1043's unseen companion must have mass $M_2 > 0.07$ M_{\odot} and orbital separation $a > 0.27$ R_{\odot} . However, we can rule out a low-mass companion on observational and physical grounds.

The radial velocities, taken alone, allow for a low mass M dwarf or perhaps a brown dwarf companion, like the recently discovered eclipsing system J1205–0242 ([Parsons et al. 2017](#); [Rappaport et al. 2017](#)). However, an M dwarf should fill the Roche lobe at this orbital separation. We see no evidence of mass transfer. An M dwarf should also out-shine the WD at infrared wavelengths. We compare publically available *GALEX* ultraviolet, SDSS optical, and UKIDSS infrared photometry to the synthetic WD spectral energy distribution and find good agreement with the WD model, and no evidence for infrared excess. The close orbital separation and lack of evidence for an M dwarf companion suggest that J1043 is a double degenerate binary.

3.4.1. Gravitational Wave Detection

Double degenerate binaries like J1043 are mHz sources of gravitational waves. The strongest sources of gravitational waves in the mHz frequency range will be directly detected by *LISA*. We use the detection calculations of Korol et al. (2017) to estimate the signal-to-noise ratio (SNR) at which J1043 might be detected by *LISA*. The signal amplitude is proportional to the gravitational wave strain of a binary times the *LISA* detector pattern function. J1630+4233, a previously discovered ELM WD binary that has an orbital frequency nearly identical to J1043 (Kilic et al. 2011b), provides an appropriate comparison. Korol et al. (2017) predict that *LISA* will detect J1630+4233 at SNR=5 in 5 years of operation.

J1043's gravitational wave strain is identical to J1630+4233 if J1043 has $M_2 = 0.38 M_\odot$. Thus *LISA* will detect J1043 at SNR=5 in 5 years of operation if its mass ratio is $M_1:M_2=1:2$. Re-calculating gravitational wave strain for different mass ratios, *LISA* will detect J1043 at SNR=3 if its mass ratio is 1:1, and at SNR=9 if its mass ratio is 1:5. J1043 is a detectable gravitational wave source for even the most pessimistic 1:1 mass ratio.

Although we do not measure the mass ratio, we expect that a degenerate companion should be more massive than the observed low mass WD. ELM WDs are understood to be the result of double common-envelope evolution, in which the ELM WD evolves last (Webbink 1984; Iben 1990; Marsh et al. 1995). The Universe is not old enough to evolve a single star into an ELM WD. Indeed, eclipsing binaries in the ELM Survey with well-determined parameters have measured mass ratios between $M_1:M_2=1:2$ and 1:5 (Brown et al. 2011; Kilic et al. 2014b).

We conclude that J1043 is a likely *LISA* verification binary. To simplify the remaining discussion, we will assume that J1043's companion has the average mass found in the rest of the ELM Survey, $M_2 = 0.76 \pm 0.25 M_\odot$ (Andrews et al. 2014; Boffin 2015; Brown et al. 2016a), and thus a mass ratio of $M_1:M_2=1:4$. This choice of M_2 corresponds to an orbital inclination of $i = 12.6^{+2.9}_{-1.8}$ deg, a gravitational merger time of $\tau = 34^{+12}_{-7}$ Myr, and a gravitational wave strain of $\log h = -21.7 \pm 0.1$. Future gravitational wave measurements will tell us the exact answer.

3.5. Eclipse Light Curve

Figure 3 presents the light curves for J0822 and J1043. J0822 shows 0.2 mag deep and ≈ 60 s long eclipses every 40.5 min, statistically identical to the orbital period derived from the radial velocity data. We do not de-

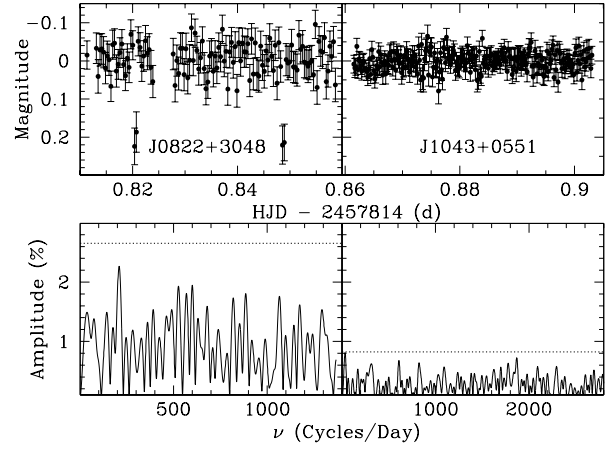


Figure 3. Light curves of J0822 and J1043 (upper panels) and their Fourier transforms (lower panels). Dotted lines are the $3\langle A \rangle$ significance limits as defined in the text. The relative photometry is available as the Data behind the Figure. J0822 shows 0.2 mag deep eclipses with a period identical to the radial velocity data.

tect the secondary eclipse. J0822 is faint, with apparent $g = 20.34$ mag, and our photometry is relatively noisy, with ± 0.04 mag errors. Because we have only 4 data points during the primary eclipse, the Fourier transform of J0822 (bottom panel) does not show significant variability above the $3\langle A \rangle$ limit, where $\langle A \rangle$ is the average amplitude up to the Nyquist frequency. The relativistic beaming effect should produce 0.35% variations at the orbital period (Shporer et al. 2010), but this is also lost in the noise in our data. Tidal distortions are not significant in J0822. The oblateness of the low mass WD is predicted to be 0.3% and the predicted amplitude of the ellipsoidal variations is $\sim 10^{-4}$, which we are unlikely to detect with ground-based observations.

The light curve and the Fourier transform for J1043 do not show any significant variability down to the $3\langle A \rangle$ limit of 0.8%. The absence of eclipses provides us with an upper limit on the inclination of the system, $i < 85.7^\circ$. Given the unknown inclination, the expected amplitudes of the relativistic beaming effect and ellipsoidal variations are $\leq 0.3\%$ and $\leq 0.15\%$, respectively. If present, these photometric signals are also lost in the noise in our observations.

We model the light curve of J0822 using JKTEBOP (Southworth et al. 2004). We use the wavelength response of the BG40 filter from Hallakoun et al. (2016) and the linear limb-darkening coefficients from Gianninas et al. (2013) to calculate the limb-darkening coefficients. We adopt gravity-darkening coefficients of 0.36 for both the primary and secondary star. We expect convection to be present in both stars, so adopting

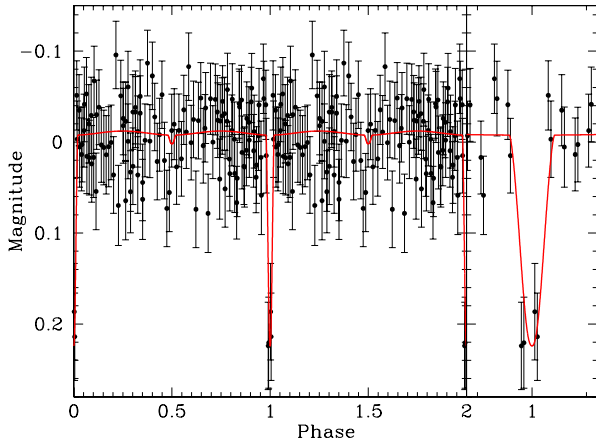


Figure 4. Light curve model of J0822 (red line) compared to the data (black dots). Orbital period and mass ratio are better constrained by the radial velocity data, so we hold those parameters fixed; the derived WD radii are consistent with model predictions for 0.3 and 0.52 M_{\odot} WDs.

$\beta = 0.36$ is reasonable. Given how sparsely our data sample the primary eclipse, we avoid using more complicated limb-darkening laws. The orbital period and the mass ratio of the system are well-constrained by the radial velocity data. We thus fix the orbital period, mass ratio, limb-, and gravity-darkening coefficients when fitting for the inclination and component radii.

Figure 4 shows the best-fit model, which has an inclination of 86.8° and reduced $\chi^2 = 0.96$. We perform 10,000 Monte Carlo simulations (Southworth et al. 2005) to estimate the errors in each parameter. Because we only have 4 data points during the primary eclipse, about half of the Monte Carlo simulations find a best-fit solution with $i < 84.5^{\circ}$. This is ruled out by the detected eclipses. Treating the radii as free parameters, a 0.22 mag eclipse depth requires $i \geq 84.5^{\circ}$ for J0822. Below $i < 84.5^{\circ}$, the model eclipse depths become too small for the observed light curve. Thus we limit the Monte Carlo simulations to the solutions with $i \geq 84.5^{\circ}$ when estimating errors. The median parameters with their errors are: $i = 88.1_{-2.3}^{+1.4}$ deg, $R_1 = 0.022_{-0.014}^{+0.015} R_{\odot}$, $R_2 = 0.0041_{-0.0037}^{+0.0082} R_{\odot}$, and $L_2/L_1 = 0.000_{-0}^{+0.038}$. Using the period determined from the radial velocity observations, the best-fit ephemeris is $T_0 = 2457814.821 \pm 0.007$ BJD_{TDB}. Note that gravitational lensing minimally affects the depth of the primary and secondary eclipses, by $< 0.6\%$ (Marsh 2001), and has not been included in our modeling.

A better light curve is, of course, desirable, but the derived parameters remain consistent with model predictions for 0.30 and 0.52 M_{\odot} WDs. The eclipsing WD binary CSS 41177 contains a $0.316 \pm 0.011 M_{\odot}$ WD with

$R = 0.02066 \pm 0.00042 R_{\odot}$ (Bours et al. 2014), very similar to J0822. Since the secondary eclipse in J0822 is not detected in our observations, the luminosity of the more massive companion star is unconstrained, but it is likely a few per cent of the luminosity of the visible WD. Multi-passband and higher signal-to-noise ratio follow-up photometry of J0822 will be useful for obtaining more precise constraints on the radii, luminosities, and temperatures of the two WDs.

Eclipsing short period systems provide excellent clocks to detect orbital decay due to gravitational waves. Hermes et al. (2012) measured $\dot{P} = -9.8 \pm 2.8 \times 10^{-12}$ s s $^{-1}$ in the 765 s eclipsing double WD binary J0651; the precision in this measurement has recently improved to better than 0.1×10^{-12} s s $^{-1}$ after 5 years of observations (J.J. Hermes, private communication). The expected \dot{P} for J0822 is about -1.4×10^{-12} s s $^{-1}$ (Piro 2011). That means J0822’s time-of-eclipse should occur 7 s earlier than expected in 5 years, and occur 30 s earlier than expected in 10 years. A reliable measurement of \dot{P} for J0822 will thus likely require a 5 to 10 year time baseline.

4. DISCUSSION

4.1. Eclipsing Double White Dwarf Binaries

There are now 7 detached, eclipsing double WD binaries known whose WD masses are directly measured. An obvious question is what happens when these double WD binaries merge due to gravitational wave radiation and begin mass transfer. Total mass is important for whether the binaries are type Ia supernova progenitors; mass ratio is important for whether the binaries will undergo stable or unstable mass transfer (e.g. Iben 1990; Han 1998; Nelemans et al. 2001a; Marsh et al. 2004; Kaplan et al. 2012).

Figure 5 plots the distribution of total mass and mass ratio of the 7 known detached, eclipsing WD binaries. M_1 is the WD that dominates the light of the binary, which is typically the lowest mass WD in the binary. Low mass WDs have larger radii and typically have higher temperatures (because they evolved more recently) than their higher mass WD companions. The only double-lined spectroscopic binary among the eclipsing systems is the equal-mass binary CSS 41177. We obtain binary parameters from the following sources: NLTT 11748 (Kaplan et al. 2014), CSS 41177 (Bours et al. 2014, 2015), GALEX J1717 (Vennes et al. 2011; Hermes et al. 2014), SDSS J0651 (Brown et al. 2011; Hermes et al. 2012), SDSS J0751 (Kilic et al. 2014b), and SDSS J1152 (Hallakoun et al. 2016). We also draw (in green) the mass distribution of

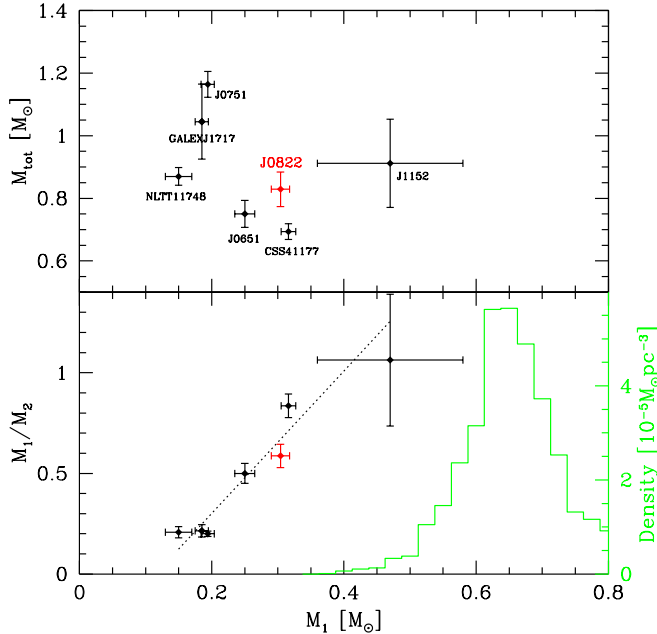


Figure 5. Total mass (upper panel) and mass ratio (lower panel) of known eclipsing double WD binaries, plotted versus mass of the most luminous WD. Green histogram is the mass distribution of WDs observed in SDSS (Kepler et al. 2016). None of the eclipsing WD binaries contain a $0.6 - 0.7 M_{\odot}$ WD of “normal” mass; a marginally significant correlation appears in mass ratio (dotted line).

DA WDs measured from the SDSS DR12 WD catalog (Kepler et al. 2016) for comparison.

Curiously, none of the eclipsing double WD binaries contain a WD that falls in the peak of the WD mass distribution observed by SDSS (green histogram, Figure 5) (Kepler et al. 2016). Rather, the eclipsing binaries all contain low mass $< 0.5 M_{\odot}$ WDs with companions that are either other low mass WDs, or else high mass $0.7 < M_2 < 1.0 M_{\odot}$ WDs for the 1:5 mass ratio systems. The total masses of the eclipsing double WD binaries range from $0.69 \pm 0.03 M_{\odot}$ to $1.16 \pm 0.04 M_{\odot}$.

The ubiquity of low mass WDs is not due to how the eclipsing double WD binaries were targeted. NLTT 11748 was targeted for its large proper motion (Kawka & Vennes 2009). CSS 41177 was identified in a search of Catalina Sky Survey light curves of $\sim 12,000$ SDSS WDs (Drake et al. 2010). GALEX J1717 was found by its ultraviolet excess and reduced proper motion (Vennes et al. 2011). SDSS J1152 was a color-selected WD candidate included in the 2-Wheeled *Kepler* continuation mission (Howell et al. 2014). Only the ELM Survey binaries were targeted for their low mass WD. Yet because low mass WDs form in compact binaries and are typically more luminous than higher-

mass WDs, binary population synthesis models predict that low mass WDs should dominate magnitude-limited samples of WD binaries (e.g. Iben 1990; Han 1998; Nelemans et al. 2001b).

However, the mass ratios of eclipsing double WD binaries are unexpected in view of binary population synthesis models. Observed mass ratios range from 1:1 to 1:5. There also appears to be a marginally significant correlation of mass ratio (and thus M_2) with M_1 , such that lower mass WDs have higher mass WD companions (as indicated by the dotted line in Figure 5). Yet models like Han (1998) and Nelemans et al. (2001b) predict predominantly 1:1.5 mass ratios for He+He WD binaries, and 1:2 to 1:3 mass ratios for He+CO WD binaries, in synthetic magnitude-limited samples of double WDs. Binaries with $M_1 \approx 0.2 M_{\odot}$ and extreme 1:5 mass ratios are missing from the models. Short-period WD binaries are sensitive to model assumptions about the stability of mass transfer and double common-envelope evolution (Toonen et al. 2014). This has implications for the likely outcomes of the mergers.

Binaries composed of He+CO WDs with mass ratios $M_1/M_2 < 0.2$ should experience stable mass transfer (Marsh et al. 2004) and evolve into AM CVn systems, a class of ultracompact binaries that consist of a WD accretor and a helium donor star (Nelemans 2005; Solheim 2010). The three eclipsing binaries with $M_1 < 0.2 M_{\odot}$ will likely evolve in this route.

He+CO WD binaries with mass ratios greater than about $M_1/M_2 > 0.5$ should experience unstable mass transfer (Marsh et al. 2004) and merge into single objects like R CrB stars (Webbink 1984; Iben 1990). The four eclipsing binaries with $M_1 > 0.25 M_{\odot}$ will likely evolve into single $\sim 0.8 M_{\odot}$ objects.

4.2. Merger Rate of Double WD Binaries

As we state above, finding double WD binaries that merge on ~ 10 Myr timescales implies many more such binaries must have formed and merged over the age of the Milky Way. In Brown et al. (2016b), we show that the distribution of ELM WD binaries in our magnitude-limited sample implies an ELM WD merger rate of $3 \times 10^{-3} \text{ yr}^{-1}$ in the Milky Way disk. The major source of uncertainty comes from the small number statistics of rapidly merging binaries like J0822 and J1043. While J0822 formally falls outside the ELM Survey color and magnitude limits, J1043 is very much a part of the sample. Assuming the prior on its secondary, J1043 ranks as the 5th shortest merger-time system in the ELM Survey after J0651, J0935, J1630, and J0106 (Figure 6).

We revisit the merger rate calculation and find that the addition of J1043 increases the estimated merger

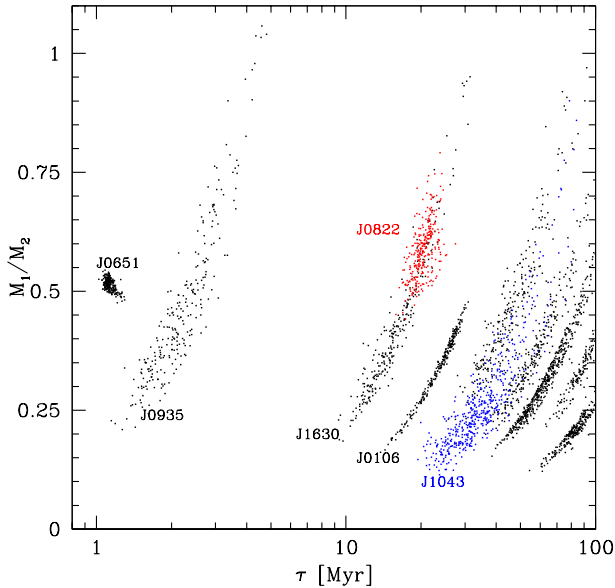


Figure 6. Gravitational wave merger time versus mass ratio for double WD binaries in the ELM Survey with $\tau < 100$ Myr. Each dot represents a Monte Carlo calculation accounting for observational uncertainties plus constraints on inclination (i.e. eclipses). J0822 is drawn in red, and J1043 is drawn in blue.

rate of ELM WD binaries in the Galactic disk by only 1%. The gain from its merger time is offset by the completeness correction (the sample is now more complete). We conclude that our sample of ELM WDs is large enough to be robust to the addition of new $\tau \sim 10$ Myr binaries; only the addition of $\tau \sim 1$ Myr binaries like J0651 and J0935 can alter the rate at the 10% level.

We also re-visit the merger rate of ELM WD binaries with extreme mass ratios, those systems that should evolve into stable mass-transfer AM CVn. J1043 is possibly one such a system. Figure 6 illustrates the mass ratio constraints on ELM Survey binaries with merger times less than 100 Myr. Every binary without an inclination measurement has a likelihood of having a mass ratio that falls in the stable mass-transfer regime. We follow Kilic et al. (2016) and estimate the merger rate from the part of the distribution that meets the Marsh et al. (2004) criteria for stable mass transfer. The uncertainties of this approach are large, but we obtain the same answer as previously published. The estimated rate is 20 to 40 times lower than the full ELM WD merger rate, depending on how the estimate is made, consistent with the AM CVn formation rate (Roelofs et al. 2007; Carter et al. 2013).

The ELM Survey samples only a subset of He+CO WD binaries, and so places only a lower limit on the Milky Way’s full He+CO WD merger rate. The fact

that an order-of-magnitude more short-period ELM WD binaries are merging than stable AM CVn binaries are forming means that most ELM WD (and thus He+CO WD) binaries experience unstable mass transfer and merge into single objects. Indeed, the ELM WD merger rate is statistically identical to the formation rate of R CrB stars in the Milky Way (Zhang et al. 2014; Karakas et al. 2015).

From a theoretical viewpoint, the conclusion that most ELM WD binaries experience unstable mass transfer is surprising. Unstable mass transfer is only expected for near-unity mass ratios. However Marsh et al. (2004) show that there remains a large region of parameter space in which the stability of mass transfer is ambiguous, in which stability depends primarily on the strength of spin-orbit coupling. When the donor ELM WD fills its Roche lobe, the accretor spins-up due to the incoming matter stream. Weak spin-orbit coupling means the accretor is unable to transfer angular momentum back to the orbit of the donor on a fast enough timescale. The result is that the binary orbit shrinks, mass transfer rate grows, and mass transfer becomes unstable. Alternatively, the initial phase of hydrogen mass-transfer may generate nova-like outbursts that drive He+CO WD systems into merger (Shen 2015). Either way, the merger rate of observed short-period ELM WD binaries like J1043 demands that mass transfer in most He+CO WD binaries is unstable.

5. CONCLUSIONS

We present the discovery of a detached eclipsing 40 min orbital period double WD binary, and a detached 46 min orbital period double WD binary. These two systems bring our targeted ELM Survey sample to 82 WD binaries. The two new systems, SDSS J082239.546+304857.19 and SDSS J104336.275+055149.90, have gravitational wave merger times of 20 Myr and ~ 34 Myr, respectively. J0822 is a detached, eclipsing double WD binary. J1043 is a likely gravitational wave verification binary.

We revisit the ELM WD binary merger rate, and find that the new discoveries affirm our previous result: observed He+CO WD binaries merge at a rate at least 40 times greater than the formation rate of stable mass-transfer AM CVn systems, and so the majority must merge into single objects like R CrB stars (Brown et al. 2016b). The implication is that spin-orbit coupling in He+CO WD mergers is very weak (Marsh et al. 2004), or else nova-like outbursts during the initial phase of mass-transfer drive the systems into merger (Shen 2015).

Eclipsing double WD binaries are especially well-constrained systems. Yet J0822 and the other 6 known

eclipsing binaries do not contain a single “normal” $0.6 M_{\odot}$ to $0.7 M_{\odot}$ WD. While four eclipsing binaries have expected mass ratios of 1:1 to 1:2, three have extreme 1:5 mass ratios in tension with binary population synthesis models. Finding and characterizing eclipsing WD binaries like J0822 is important for better understanding WD binary evolution and constraining the final outcome of WD binary mergers.

We thank B. Kunk, E. Martin, and A. Milone for their assistance with observations obtained at the MMT Observatory. This research makes use the SAO/NASA

Astrophysics Data System Bibliographic Service. This project makes use of data products from the Sloan Digital Sky Survey, which is managed by the Astrophysical Research Consortium for the Participating Institutions. This work was supported in part by the Smithsonian Institution, and in part by the NSF and NASA under grants AST-1312678 and NNX14AF65G.

Facilities: MMT (Blue Channel Spectrograph), ARC (Agile Camera)

Software: IRAF (Tody 1986, 1993), RVSAO (Kurtz & Mink 1998), JKTEBOP (Southworth et al. 2004)

REFERENCES

- Althaus, L. G., Camisassa, M. E., Miller Bertolami, M. M., Córscico, A. H., & García-Berro, E. 2015, *A&A*, 576, A9
- Althaus, L. G., Miller Bertolami, M. M., & Córscico, A. H. 2013, *A&A*, 557, A19
- Altmann, M., Roeser, S., Demleitner, M., Bastian, U., & Schilbach, E. 2017, *A&A*, 600, L4
- Andrews, J. J., Price-Whelan, A. M., & Agüeros, M. A. 2014, *ApJL*, 797, L32
- Boffin, H. M. J. 2015, *A&A*, 575, L13
- Bours, M. C. P., Marsh, T. R., Gänsicke, B. T., & Parsons, S. G. 2015, *MNRAS*, 448, 601
- Bours, M. C. P., Marsh, T. R., Parsons, S. G., et al. 2014, *MNRAS*, 438, 3399
- Bragaglia, A., Greggio, L., Renzini, A., & D’Odorico, S. 1990, *ApJL*, 365, L13
- Breedt, E., Steeghs, D., Marsh, T. R., et al. 2017, *MNRAS*, 468, 2910
- Brown, W. R., Gianninas, A., Kilic, M., Kenyon, S. J., & Allende Prieto, C. 2016a, *ApJ*, 818, 155
- Brown, W. R., Kilic, M., Allende Prieto, C., Gianninas, A., & Kenyon, S. J. 2013, *ApJ*, 769, 66
- Brown, W. R., Kilic, M., Allende Prieto, C., & Kenyon, S. J. 2012, *ApJ*, 744, 142
- Brown, W. R., Kilic, M., Hermes, J. J., et al. 2011, *ApJL*, 737, L23
- Brown, W. R., Kilic, M., Kenyon, S. J., & Gianninas, A. 2016b, *ApJ*, 824, 46
- Carter, P. J., Marsh, T. R., Steeghs, D., et al. 2013, *MNRAS*, 429, 2143
- Chiba, M. & Beers, T. C. 2000, *AJ*, 119, 2843
- Drake, A. J., Beshore, E., Catelan, M., et al. 2010, *ArXiv e-print*, 1009.3048
- Gianninas, A., Bergeron, P., & Ruiz, M. T. 2011, *ApJ*, 743, 138
- Gianninas, A., Dufour, P., Kilic, M., et al. 2014, *ApJ*, 794, 35
- Gianninas, A., Kilic, M., Brown, W. R., Canton, P., & Kenyon, S. J. 2015, *ApJ*, 812, 167
- Gianninas, A., Strickland, B. D., Kilic, M., & Bergeron, P. 2013, *ApJ*, 766, 3
- Hallakoun, N., Maoz, D., Kilic, M., et al. 2016, *MNRAS*, 458, 845
- Han, Z. 1998, *MNRAS*, 296, 1019
- Hermes, J. J., Gänsicke, B. T., Koester, D., et al. 2014, *MNRAS*, 444, 1674
- Hermes, J. J., Kilic, M., Brown, W. R., et al. 2012, *ApJL*, 757, L21
- Howell, S. B., Sobeck, C., Haas, M., et al. 2014, *PASP*, 126, 398
- Iben, Jr., I. 1990, *ApJ*, 353, 215
- Istrate, A. G., Marchant, P., Tauris, T. M., et al. 2016, *A&A*, 595, A35
- Kaplan, D. L., Bhalariao, V. B., van Kerkwijk, M. H., et al. 2013, *ApJ*, 765, 158
- Kaplan, D. L., Bildsten, L., & Steinfadt, J. D. R. 2012, *ApJ*, 758, 64
- Kaplan, D. L., Marsh, T. R., Walker, A. N., et al. 2014, *ApJ*, 780, 167
- Karakas, A. I., Ruiter, A. J., & Hampel, M. 2015, *ApJ*, 809, 184
- Kawka, A. & Vennes, S. 2009, *A&A*, 506, L25
- Kenyon, S. J. & Garcia, M. R. 1986, *AJ*, 91, 125
- Kepler, S. O., Pelisoli, I., Koester, D., et al. 2016, *MNRAS*, 455, 3413
- Kilic, M., Brown, W. R., Allende Prieto, C., Kenyon, S. J., & Panei, J. A. 2010, *ApJ*, 716, 122
- Kilic, M., Brown, W. R., Allende Prieto, C., et al. 2011a, *ApJ*, 727, 3

- Kilic, M., Brown, W. R., Gianninas, A., et al. 2014a, *MNRAS*, 444, L1
- . 2017, *MNRAS*, accepted
- Kilic, M., Brown, W. R., Heinke, C. O., et al. 2016, *MNRAS*, 460, 4176
- Kilic, M., Brown, W. R., Hermes, J. J., et al. 2011b, *MNRAS*, 418, L157
- Kilic, M., Hermes, J. J., Gianninas, A., et al. 2014b, *MNRAS*, 438, L26
- Korol, V., Rossi, E. M., Groot, P. J., et al. 2017, *MNRAS*, 470, 1894
- Kraft, R. P., Mathews, J., & Greenstein, J. L. 1962, *ApJ*, 136, 312
- Kurtz, M. J. & Mink, D. J. 1998, *PASP*, 110, 934
- Marsh, T. R. 2001, *MNRAS*, 324, 547
- . 2011, *Classical and Quantum Gravity*, 28, 094019
- Marsh, T. R., Dhillon, V. S., & Duck, S. R. 1995, *MNRAS*, 275, 828
- Marsh, T. R., Nelemans, G., & Steeghs, D. 2004, *MNRAS*, 350, 113
- Maxted, P. F. L., Marsh, T. R., & Moran, C. K. J. 2000, *MNRAS*, 319, 305
- Morales-Rueda, L., Marsh, T. R., Maxted, P. F. L., et al. 2005, *MNRAS*, 359, 648
- Moran, C., Marsh, T. R., & Bragaglia, A. 1997, *MNRAS*, 288, 538
- Mukadam, A. S., Owen, R., Mannery, E., et al. 2011, *PASP*, 123, 1423
- Nelemans, G. 2005, in *Astronomical Society of the Pacific Conference Series*, Vol. 330, *The Astrophysics of Cataclysmic Variables and Related Objects*, ed. J.-M. Hameury & J.-P. Lasota, 27
- Nelemans, G. 2009, *Classical and Quantum Gravity*, 26, 094030
- Nelemans, G., Napiwotzki, R., Karl, C., et al. 2005, *A&A*, 440, 1087
- Nelemans, G., Portegies Zwart, S. F., Verbunt, F., & Yungelson, L. R. 2001a, *A&A*, 368, 939
- Nelemans, G., Yungelson, L. R., Portegies Zwart, S. F., & Verbunt, F. 2001b, *A&A*, 365, 491
- Nissanke, S., Vallisneri, M., Nelemans, G., & Prince, T. A. 2012, *ApJ*, 758, 131
- Parsons, S. G., Hermes, J. J., Marsh, T. R., et al. 2017, *MNRAS*, submitted
- Parsons, S. G., Marsh, T. R., Gänsicke, B. T., Drake, A. J., & Koester, D. 2011, *ApJL*, 735, L30
- Piro, A. L. 2011, *ApJL*, 740, L53
- Rappaport, S., Vanderburg, A., Nelson, L., et al. 2017, *ApJ*, submitted
- Rebassa-Mansergas, A., Parsons, S. G., García-Berro, E., et al. 2017, *MNRAS*, 466, 1575
- Roelofs, G. H. A., Nelemans, G., & Groot, P. J. 2007, *MNRAS*, 382, 685
- Saffer, R. A., Liebert, J., & Olszewski, E. W. 1988, *ApJ*, 334, 947
- Schönrich, R., Binney, J., & Dehnen, W. 2010, *MNRAS*, 403, 1829
- Shen, K. J. 2015, *ApJL*, 805, L6
- Shporer, A., Kaplan, D. L., Steinfadt, J. D. R., et al. 2010, *ApJL*, 725, L200
- Solheim, J. 2010, *PASP*, 122, 1133
- Southworth, J., Maxted, P. F. L., & Smalley, B. 2004, *MNRAS*, 351, 1277
- Southworth, J., Smalley, B., Maxted, P. F. L., Claret, A., & Etzel, P. B. 2005, *MNRAS*, 363, 529
- Steinfadt, J. D. R., Kaplan, D. L., Shporer, A., Bildsten, L., & Howell, S. B. 2010, *ApJL*, 716, L146
- Tody, D. 1986, in *Proc. SPIE*, Vol. 627, *Instrumentation in astronomy VI*, ed. D. L. Crawford (Bellingham, WA:SPIE), 733
- Tody, D. 1993, in *ASP Conf. Ser.* Vol. 52, *Astronomical Data Analysis Software and Systems II*, ed. R. J. Hanisch, R. J. V. Brissenden, & J. Barnes (San Francisco: ASP), 173
- Toonen, S., Claeys, J. S. W., Mennekens, N., & Ruiter, A. J. 2014, *A&A*, 562, A14
- Tremblay, P.-E. & Bergeron, P. 2009, *ApJ*, 696, 1755
- Tremblay, P.-E., Gianninas, A., Kilic, M., et al. 2015, *ApJ*, 809, 148
- Vennes, S., Thorstensen, J. R., Kawka, A., et al. 2011, *ApJL*, 737, L16
- Webbink, R. F. 1984, *ApJ*, 277, 355
- Zhang, X., Jeffery, C. S., Chen, X., & Han, Z. 2014, *MNRAS*, 445, 660